Nano Energy (2014) **10**, 135–143

Available online at www.sciencedirect.com

ScienceDirect

journal homepage: www.elsevier.com/locate/nanoenergy

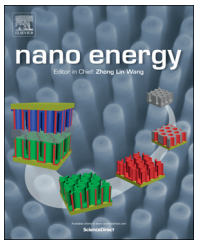

RAPID COMMUNICATION

Morphology and composition controlled platinum-cobalt alloy nanowires prepared by electrospinning as oxygen reduction catalyst

Drew C. Higgins, Rongyue Wang, Md. Ariful Hoque, Pouyan Zamani, Salah Abureden, Zhongwei Chen*

Department of Chemical Engineering, Waterloo Institute for Nanotechnology, Waterloo Institute of Sustainable Energy, University of Waterloo, 200 University Avenue W, Waterloo, ON, Canada N2L 3G1

Received 6 May 2014; received in revised form 22 August 2014; accepted 11 September 2014
Available online 22 September 2014

KEYWORDS
Oxygen reduction;
Fuel cells;
Electrocatalysis;
Electrospinning;
Nanowires

Abstract
One-dimensional platinum-cobalt alloy nanowires (PtCoNWs) are prepared by electrospinning, which provides a versatile platform for the synthesis of nanowires with tunable diameters and atomic compositions. PtCoNWs with a near unity stoichiometric ratio, excellent atomic distribution and an average diameter of 28 nm were evaluated for oxygen reduction reaction (ORR) activity in 0.1 M $HClO_4$ electrolyte. Over a four-fold enhancement in Pt mass-based activity at an electrode potential of 0.9 V vs. RHE is obtained in comparison to pure PtNWs, highlighting the beneficial impact of the alloying structure. A near 7-fold specific activity increase is also observed in comparison to commercial Pt/C catalyst, along with improved electrochemically active surface area retention through repetitive (1000) potential cycles. Electrospinning is thereby an attractive approach to prepare morphology and composition controlled PtCoNWs that could potentially one day replace conventional nanoparticle catalysts.

Introduction

Operating with high efficiency and zero emissions, polymer electrolyte membrane fuel cells (PEMFCs) are considered among the most promising clean energy conversion technologies for a variety of applications, including transportation and stationary power generation. The widespread commercial success of PEMFCs is however still hindered by two primary technical challenges: the high system costs and poor operational durability. Of the overall fuel cell stack cost, the high surface area carbon supported platinum

*Corresponding author. Tel.: +1 519 888 4567x38664.
E-mail address: zhwchen@uwaterloo.ca (Z. Chen).

http://dx.doi.org/10.1016/j.nanoen.2014.09.013
2211-2855/

nanoparticle (Pt/C) catalysts comprise over 30% [1], with the majority of Pt content required at the cathode to catalyze the inherently sluggish oxygen reduction reaction (ORR). Additionally, the harsh oxidizing conditions lead to significant deterioration of Pt/C by carbon support corrosion and Pt nanoparticle surface area loss by agglomeration or dissolution [2-4]. This results in detrimental performance loss and PEMFC system reliability that falls significantly short of the 5000 h operational lifetime target set by the Department of Energy [5].

To address these challenges, significant research efforts have focused on the development of new ORR catalyst technologies that can either reduce or eliminate the amount of Pt required at the cathode [6-8]. While great progress has been realized towards the development of non-precious metal based catalyst technologies [9,10], this approach remains a long term objective, owing primarily to significant shortcomings in terms of operational durability. Therefore the development of highly stable Pt-based catalysts that can provide improved ORR activity represents the most viable solution [11], as it will allow for reduced Pt contents to achieve practical fuel cell performance. This likely requires a fundamental shift from conventional zero-dimensional Pt nanoparticle based systems to new catalyst designs and architectures, which has been a focus of recent research endeavors [12-17].

To this end, one-dimensional (1D) Pt and Pt-alloy catalysts are considered promising cathode catalysts for PEMFC technologies [18-23]. Increased activity is commonly observed on this new paradigm of nanostructured catalysts [24-26], owing to the relatively smooth surfaces on the atomic scale that consist of Pt atoms with high coordination numbers. This effectively weakens the adsorption strengths of oxygen species on Pt, thereby reducing overpotentials for the ORR. These smooth Pt surfaces also have reduced surface energies, rendering them less prone to activity loss by dissolution and agglomeration during PEMFC operation; and their self-supported nature can eliminate the detrimental impact of carbon corrosion. Even further activity enhancements can be realized by effectively coupling 1D nanostructure control strategies with Pt-alloying using relatively inexpensive transition metals such as Fe, Co and Ni [27-30]. Understanding and optimizing the exact structural and compositional factors underlying the performance of 1D Pt-alloy catalysts however still remains a challenge [31], yet holds promise to generate improved catalysts that can perpetuate the technological advancement of PEMFC systems. Establishing reliable techniques in order to prepare Pt and Pt-alloy nanowires with readily controllable diameters and atomic compositions is desirable, and would provide a versatile platform for both fundamental and practical investigations in order to develop unique catalyst systems with excellent activity and stability towards the ORR.

Electrospinning has been used as an effective technique to prepare a wide array of nanowire and nanofiber structures including metal oxides [32], non-precious metal ORR catalysts [33,34] and Pt-based materials [33,35]. In the present study, using Co as the choice alloying element owing to the high activity of Pt_3Co surfaces towards the ORR [36], we report the first development of PtCo nanowires (PtCoNW) by the electrospinning technique. PtCoNWs with near unity stoichiometric ratios were investigated for ORR activity by half-cell electrochemical evaluation, and were found to provide significantly improved Pt-mass and surface area specific activities in comparison to commercial Pt/C and pure PtNWs. Catalyst surface area retention of PtCoNWs during electrochemical cycling was also improved in comparison to commercial Pt/C, highlighting their promise as ORR electrocatalysts for PEMFC applications. We furthermore demonstrate the versatility of the electrospinning process in order to prepare PtCoNWs with varying Pt:Co stoichiometric ratios and nanowire diameters, providing a valuable platform for future studies in order to elucidate and optimize the effects of 1D nanostructure, chemical composition and atomic distributions on ORR activity.

Materials and methods

PtCoNW fabrication

Platinum-cobalt nanowires (PtCoNW) were prepared by electrospinning a methanol/water solution of polyvinylpyrrolidone (PVP, MW=1,300,000), hexachloroplatinic acid hexahydrate and cobalt acetate tetrahydrate. The use of cobalt acetate tetrahydrate could also be substituted for cobalt nitrate with no changes observed to the nanofiber morphology. In a typical process, 34.9 mg of PVP was dissolved in 0.9 mL of methanol, and 18.75 mg of hexachloroplatinic acid hexahydrate and 8.15 mg of cobalt acetate tetrahydrate were dissolved in 0.1 mL of DDI water. These values correspond to a precursor solution containing 4 wt% PVP, 3 wt% metal salts, and a Pt to Co molar ratio of 53:47 that were used as the standard in the present study. It was necessary to use water as a co-solvent to eliminate precipitation of PVP in methanol solution upon addition of the metal precursor salts. The prepared DDI water solution was then added to the methanol/PVP solution, and the entire mixture was stirred magnetically for 1 h. This solution was then loaded into a syringe with a stainless steel tip for subsequent electrospinning.

The electrospinning process was carried out inside an acrylic chamber, and in order to ensure successful nanofiber formation, it was necessary to decrease the relative humidity to below ca. 40% by introducing dry nitrogen gas. The syringe tip was stationed 6 cm from the aluminum foil collection substrate and the power source was set to 6 kV. The solution flow rate was set to 0. 25 mL h^{-1}, during which time a beige film formed on the aluminum foil surface. After completion, the electrospun film was peeled off the aluminum foil and loaded into a 0.5 in. diameter quartz tube. This tube was then loaded into a large tube furnace and the temperature was increased to 480 °C at a heating rate of 0.5 °C min^{-1}. After removal of PVP, the resultant black materials were collected, and subjected to hydrogen treatment in a tube furnace at 150 °C for 2 h, and the resultant PtCoNWs were collected for subsequent characterization.

Physicochemical characterization

Scanning electron microscopy (SEM) was carried out on a LEO FESEM 1530, and TEM images were collected on a JEOL 2010F equipped with electron diffraction imaging and x-ray analysis capabilities. X-ray diffraction patterns (XRD) were

collected on an Inel XRG 300 diffractometer using a Cu x-ray source. Inductively coupled plasma (ICP) spectroscopy was conducted using a Teledyne Leeman Labs Prodigy High Dispersion ICP system. Atomic concentrations were evaluated by digesting PtCoNW powder in an aqua regia solution. Measurements were done in triplicates, and the obtained spectra were calibrated with respect to two separate commercial standard solutions to ensure accuracy.

Electrochemical characterization

PtCoNW catalyst ink was prepared by mixing 3 mg of PtCoNWs and 3 mg of Vulcan XC-72 carbon black in 2 mL of ethanol containing 4 μL of 15 wt% Nafion solution. 10 μL of the prepared catalyst ink solution was then deposited onto a polished glassy carbon disc electrode (geometric surface area of 0.19635 cm^{-2}) leading to a loading of 59.9 $\mu g_{Pt}\ cm^{-2}$, and allowed to completed dry under ambient conditions. The electrode was them immersed into 0.1 M $HClO_4$ maintained at 30 °C by a circulating water bath, and all electrochemical testing was carried out using a reference hydrogen electrode (RHE) and a platinum wire counter electrode. In order to evaluate oxygen reduction reaction (ORR) activity, the potential of the electrode was scanned at 10 mV s^{-1} in the positive direction under oxygen saturated electrolyte conditions and at electrode rotation rates varying from 100 to 1600 rpm. In order to remove capacitative contributions, background currents obtained under the same conditions except for with nitrogen saturation were removed, and the resultant ORR current densities were corrected for uncompensated electrolyte resistances using a technique reported previously [37]. Accelerated degradation testing (ADT) was conducted by repeatedly cycling the electrode potential from 0.05 to 1.3 V vs. RHE at a scan rate of 50 mV s^{-1}. Electrochemically active surface area estimates were determined by the H_{upd} technique [38]. Commercial carbon supported platinum (Pt/C, TKK) was tested for comparison using an electrode loading of 20 $\mu g_{Pt}\ cm^{-2}$, a commonly utilized value for high surface area commercial Pt catalysts [39].

Results and discussion

PtCoNWs were prepared by electrospinning a solution containing PVP as the carrier polymer, owing to its ability to complex with metal salt precursors. To produce long, uniform nanofibers, the metal salt concentration was maintained at 3 wt% and an optimal PVP concentration of 4 wt% was determined systematically through scanning electron microscopy (SEM) imaging of the prepared materials (Figure S1). We found that by varying the concentration of metal salts added into the solution between 1 and 5 wt%, no changes to the as prepared PtCo–PVP nanofibers were observed (Figure 1); however after PVP removal, significant variations in the average PtCoNW diameters occurred (Figure 2). At 1 wt% metal salt, no nanowires were obtained (not shown), indicating that the concentration of Pt and Co in the PtCo–PVP nanofibers was too low to achieve good interconnectivity during heat treatment. Increasing the metal salt concentration from 2 to 5 wt% resulted in an increase in the average nanowire diameters from 24 to 41 nm, in a near linear fashion (Figure 2c, inset). Unless specified otherwise, as the standard for subsequent investigations, PtCoNWs were prepared with a metal salt concentration of 3 wt%, PVP concentration of 4 wt% and a Pt:Co atomic ratio of 53:47. Additionally, a sufficiently slow rate of temperature increase (0.5 °C/min) for PVP removal was necessary, as higher rates of temperature increase would result in the nanowires melting together into 3-dimensional agglomerate structures (Figure S2).

TEM images of PtCoNWs after PVP removal and hydrogen reduction are displayed in Figure 3a and b. Nanowires with micrometer scale length and an average diameter of ca. 28 nm are clearly observed, and a polycrystalline structure was indicated by the select area electron diffraction (SAED) patterns (Figure 3b, inset) and high resolution TEM (Figure 3c). After PVP removal, both Pt (fcc) and Co_3O_4 (cubic) crystalline phases were observed by XRD (Figure 3d). After hydrogen treatment at 150 °C, disappearance of the Co_3O_4 peaks was observed and the Pt(fcc) peak locations were shifted to higher diffraction angles indicating the successful incorporation of Co into the Pt-alloy phase structure [40,41]. Both Pt and Co were well distributed throughout the entirety of the PtCoNWs evidenced by electrode dispersive x-ray (EDX) color mapping (Figure 3e). The overall EDX spectra is displayed in Figure S3, indicating a Pt:Co ratio of approximately 54:46, in close agreement with the 53:47 ratio used in the electrospinning solution. ICP analysis on a bulk sample of nanowires confirmed these results, showing that the PtCoNWs are composed of 52.96 at% Pt and 47.04 at% Co.

It was also possible to prepare PtCo–PVP nanofibers with readily tunable Pt:Co atomic contents, along with pure Pt–PVP nanofibers. SEM images of Pt–PVP, $Pt_{53}Co_{47}$–PVP, $Pt_{36}Co_{64}$–PVP and $Pt_{27}Co_{73}$–PVP nanofibers are displayed in Figure 4a, b, c and d, respectively. Consistent nanofiber morphology, diameters and uniformity are observed, highlighting once again the versatility of the PtCoNW electrospinning process. Drawing on this, the Pt–PVP nanofibers were heat treated in air to produce pure PtNWs for comparative purposes, with TEM and high resolution TEM images provided in Figure 4e and f, respectively. Like PtCoNWs, PtNWs displayed a polycrystalline structure as highlighted by the SAED pattern provided in Figure 4e (inset). The EDX spectra (Figure S4) indicated the atomic purity of the PtNWs. It should also be noted that for pure PtNWs, a relatively lower heat treatment temperature of 450 °C was used to remove PVP. In the case of PtCoNWs however, at this slightly lower temperature, residual PVP remained on the surface of the nanowires as evidenced by TEM imaging (Figure S5) and large oxidative currents observed during electrochemical testing at potentials above ca. 0.6 V vs. RHE. This indicates some sort of interaction occurring between PVP and the cobalt precursors, and is also evidenced by the thermogravimentric analysis (TGA) where a very minor weight loss is observed for the Co containing samples in this 400–480 °C temperature range (Figure S6). To overcome this challenge, a slightly increased PVP removal temperature of 480 °C was utilized for PtCoNW preparation.

ORR activities of the nanowire samples were investigated by electrochemical half-cell testing in 0.1 M $HClO_4$ at 30 °C. The PtCoNW electrode preparation process was investigated and optimized, whereby Figure S7 provides insight into the various parameters (electrode loading, carbon incorporation) that must

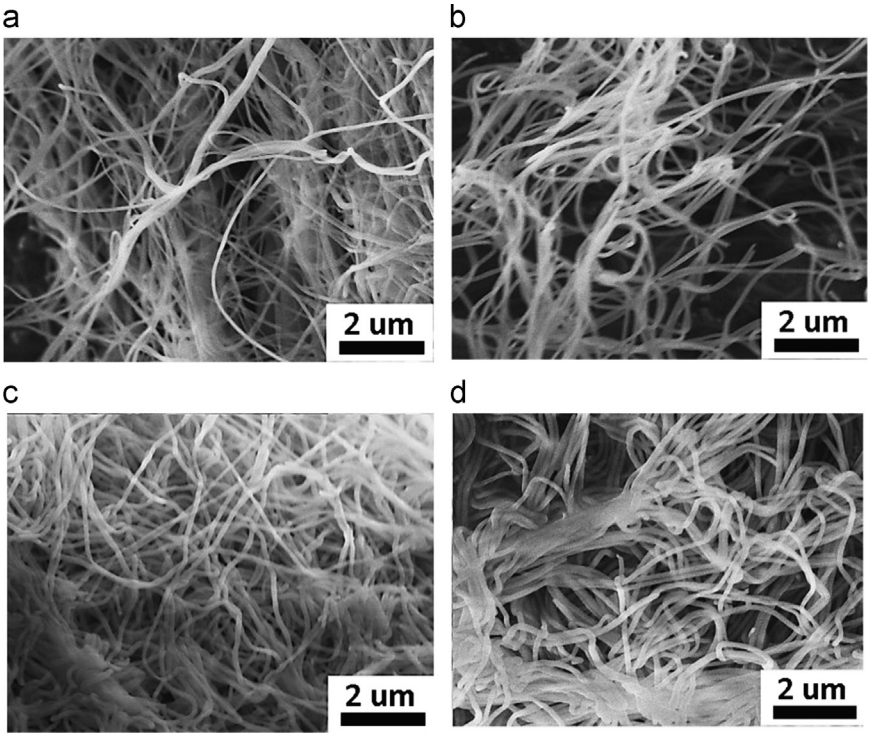

Figure 1 SEM images of PtCo-PVP nanofibers prepared with (a) 1, (b) 2, (c) 4 and (d) 5 wt% metal salts in the precursor solution. For PtCo-PVP nanofibers electrospun with 3 wt% metal salt precursor solution please refer to Figure 4b.

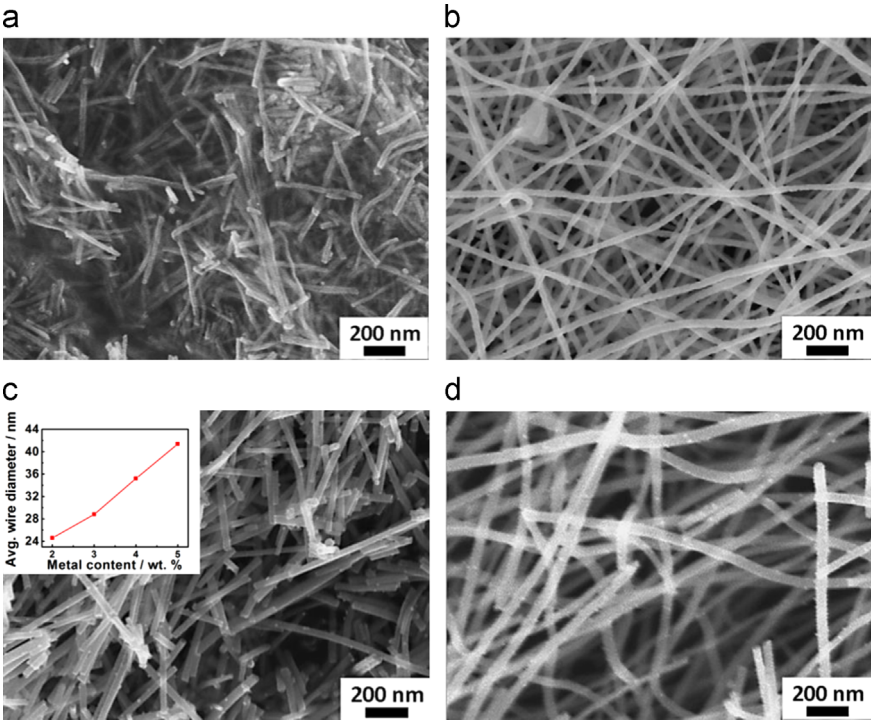

Figure 2 SEM images of PtCoNWs prepared using metal salt concentrations in the precursor solution of (a) 2, (b) 3, (c) 4 and (d) 5 wt%. (c-inset) Plot of average nanowire diameter vs. metal content of precursor solution.

be considered when dealing with extended surface Pt nanostructures [42]. Following background current and uncompensated electrolyte resistance correction [37], Figure 5a provides performance evaluation of PtNW and PtCoNW at electrode metal loadings of 76.4 $\mu g\,cm^{-2}$ and catalyst to carbon black weight ratios of 1:1 (morphology depicted in Figure S8). Notably, PtCoNWs demonstrate an on-set potential and half-wave potential of 1.01 and 0.92 V vs. RHE, respectively, representing 40 mV increases over that of PtNW. These activity enhancements are observed despite a lower overall

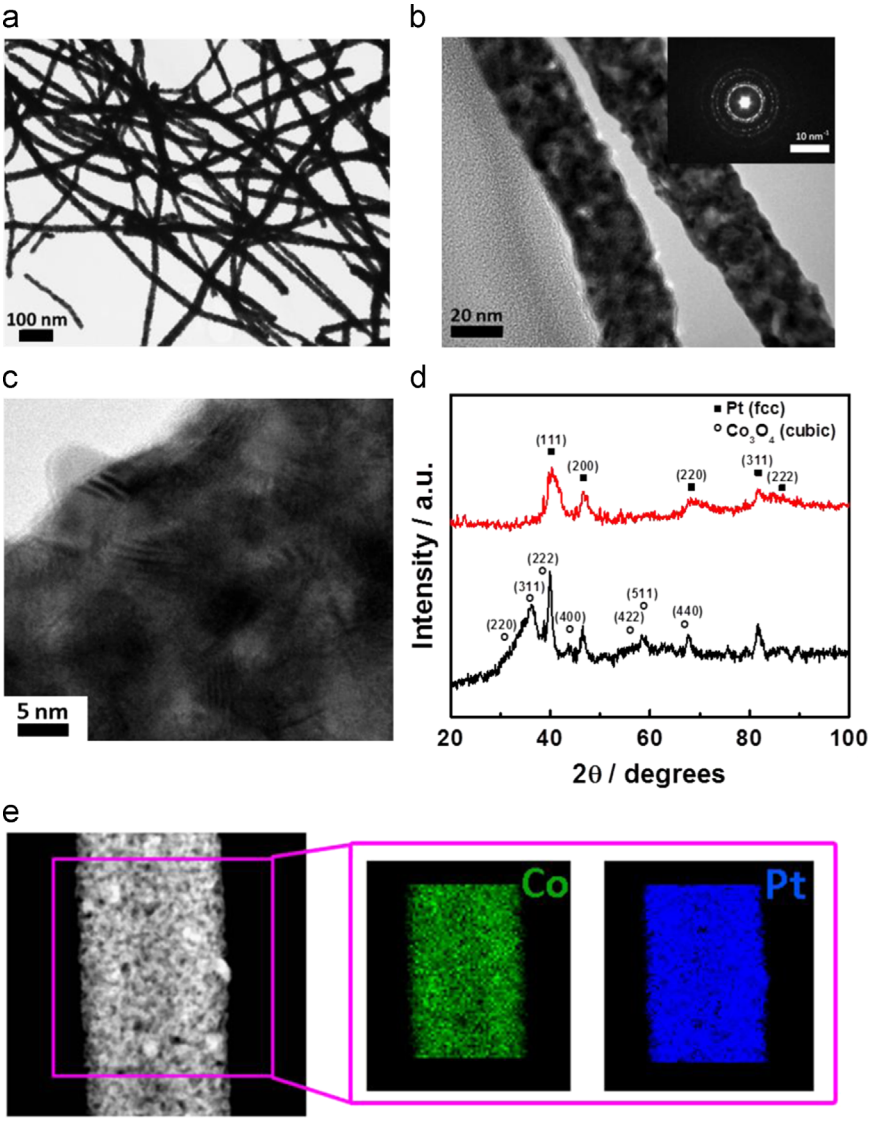

Figure 3 (a,b) TEM, (c) high resolution TEM images and (b-inset) SAED patterns of PtCoNWs. (d) XRD diffraction pattern of (black) PtCoNWs before and (red) after reduction in hydrogen at 150 °C. (d) EDX color map of PtCoNWs.

Pt electrode loading for PtCoNW (59.9 $\mu g_{Pt}\ cm^{-2}$), highlighting the dramatic activity gains realized by alloying Pt with Co atoms. The increase in ORR activity of the PtCoNWs can most likely be attributed to the modified electronic and structural properties of alloy surfaces in comparison to pure Pt [43]. These modulated features in turn tune the adsorptive properties of the catalytically active surface structure, weakening the binding with spectator oxygen containing species (i.e., OH_{ad}), thereby freeing up more active sites for the ORR and enhancing the reaction kinetics [36]. Additional ORR activity improvements for PtCoNWs are realized by the partial replacement of expensive Pt atoms in the nanowire core, reducing the catalytically active Pt content that is not accessible to reactant oxygen species. ORR polarization plots for PtCoNWs and PtNWs at electrode rotation rates varying from 100 to 1600 rpm are also provided in Figure S9.

Figure 5**b** provides the ORR performance of PtCoNWs in comparison to commercial Pt/C with a lower electrode loading of 20 $\mu g_{Pt}\ cm^{-2}$, a value typically used for commercial catalyst testing [39]. To account for different mass loadings of Pt on the electrode and provide quantitative evaluation, Tafel plots displaying mass-transport corrected kinetic current densities (i_k) [44] on a Pt mass basis are provided in Figure 5**c**. Figure 5**d** also provides the calculated Pt-based mass and specific activities of PtCoNWs and Pt/C evaluated at 0.9 V vs. RHE. Notably, PtCoNWs demonstrate a specific activity of 1.6 mA cm_{Pt}^{-2}, an almost 7-fold improvement in comparison to commercial Pt/C (0.23 mA cm_{Pt}^{-2}). In addition to these significant specific activity improvements arising from the previously discussed alloy configuration, it is highly likely that the anisotropic nanostructure of the PtCoNWs provides distinct performance advantages as well. Extended surface structures such as nanowires have a larger portion of high coordination number surface atoms in comparison to zero-dimensional nanoparticles with numerous low coordinated surface atoms and defects. The elongated nanowire structure therefore provides a relatively smooth surface that can mimic the extended surface structure of bulk polycrystalline films, enhancing the ORR kinetics of the catalyst by supressing the adsorption of active site blocking spectator species [30,31]. At

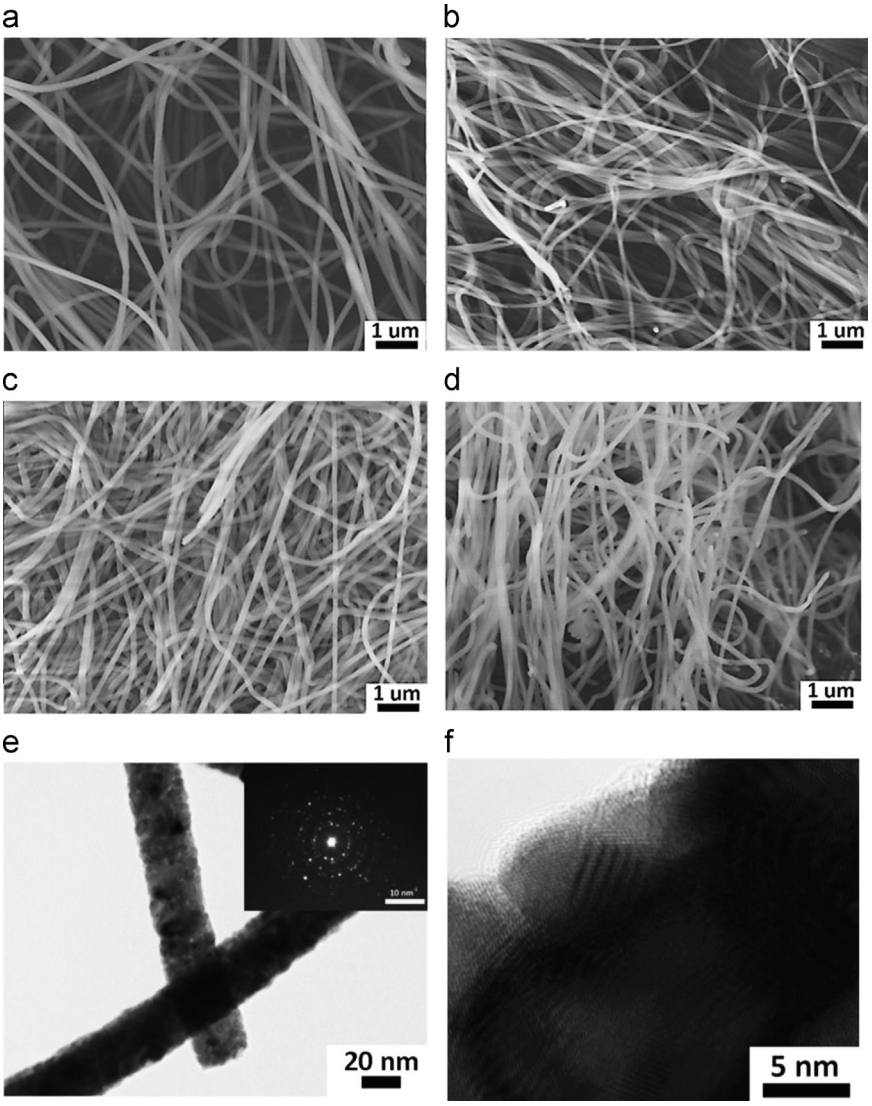

Figure 4 SEM images of (a) Pt-PVP, (b) $Pt_{53}Co_{47}$-PVP, (c) $Pt_{36}Co_{64}$-PVP and (d) $Pt_{27}Co_{73}$-PVP nanowires. (e) TEM and (f) high resolution TEM images of PtNWs, with (e-inset) SAED pattern.

all current densities evaluated, PtCoNWs also provide higher Pt mass based activities than commercial Pt/C, including a 65% improvement at 0.9 V vs. RHE (200 mA mg_{Pt}^{-1} vs. 121 mA mg_{Pt}^{-1}, respectively). It should also be noted that using lower electrode loadings of PtCoNW could result in higher Pt-mass based activities. Performance as high as 260 mA mg_{Pt}^{-1} was obtained at an electrode loading of 29.9 μg_{Pt} cm^{-2} (900 rpm, Figure S7a), most likely due to increased catalyst utilization under these conditions. Achieving the theoretical mass-transport limited current densities predicted by the Levich equation (ca. 4.3 at 900rpm, 5.7 at 1600 rpm) were however not possible at lower catalyst loadings owing to incomplete electrode coverage, an observation consistent with previous findings [45] and inherent with relatively low surface area catalysts.

The stability of PtCoNW was investigated by electrochemical accelerated degradation testing (ADT). The potential of the electrode was swept 1000 times between 0.05 and 1.3 V vs. RHE at 50 mV s^{-1} with the electrolyte temperature maintained at 30 °C (Figure 5e). Electrochemically active surface areas (ECSAs) were determined by measuring the charge transfer for hydrogen adsorption/desorption [38]. Figure 5f provides the normalized ECSA remaining as a function of cycle number. After 1000 cycles, PtCoNWs retained 75% of the initial ECSA, compared to 59% for commercial Pt/C. This indicates that the extended surface mimetic structure of PtCoNWs can potentially mitigate Pt dissolution and agglomeration in addition to overcoming the detrimental impact of carbon corrosion owing to the their self-supported nature.

Conclusions

In summary, PtCoNWs were prepared by electrospinning and found to provide excellent activity and stability towards the ORR in acidic electrolytes. The benefits of alloying were demonstrated by comparing the activity of PtCoNWs with that of pure PtNWs, whereby over a 4 × improvement in Pt mass-based activities at 0.9 V vs. RHE was achieved with the incorporation of Co into the 1D Pt nanostructure. An almost 7-fold improvement in specific activity was observed for

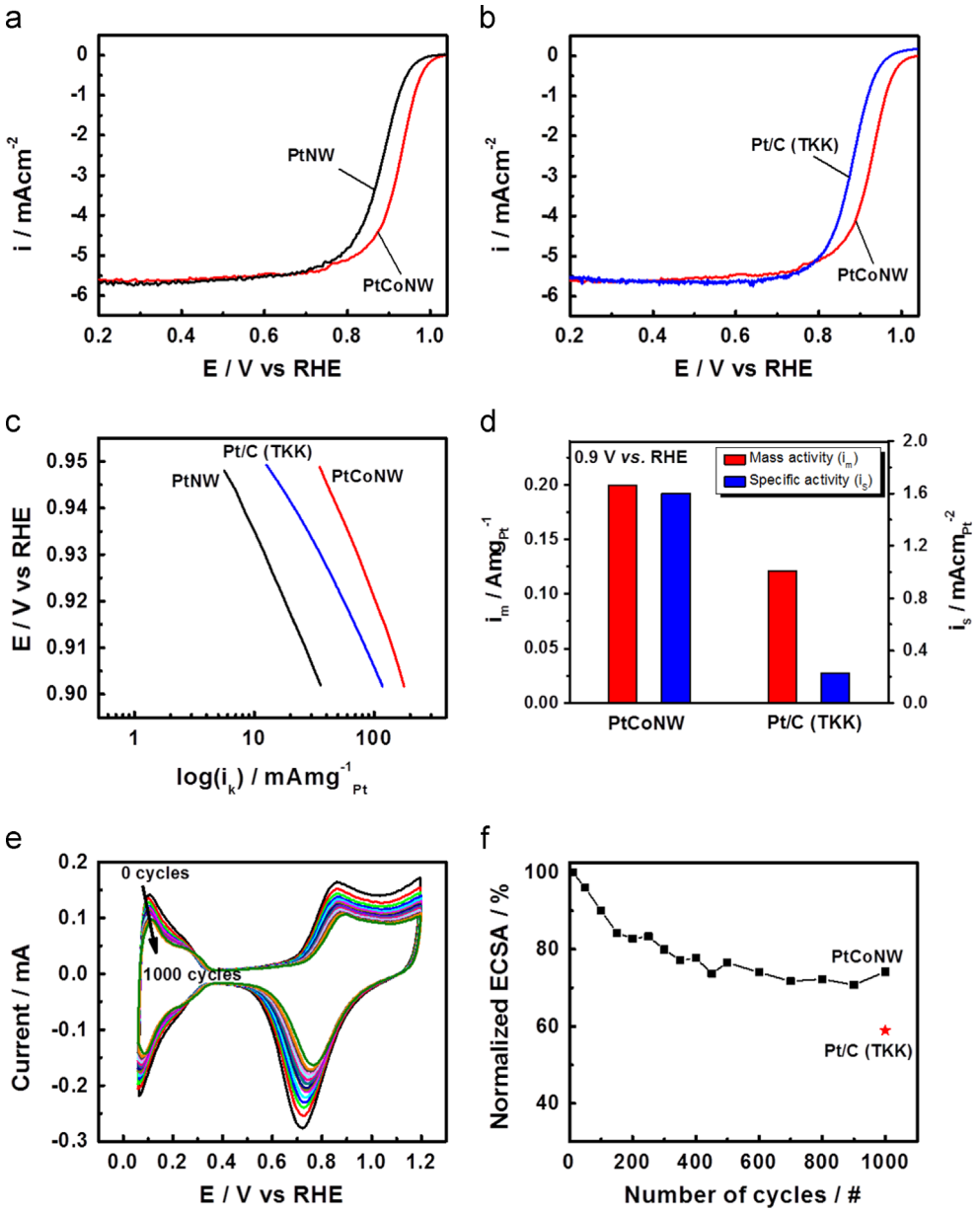

Figure 5 RDE polarization curves for (a) PtCoNW and PtNW and (b) PtCoNW and commercial Pt/C in 0.1 M $HClO_4$. (c) Mass-transport corrected Tafel plots for all materials on a Pt-mass basis and (c-inset) determined Pt-based mass and specific based activities at 0.9 V vs. RHE for PtCoNW and Pt/C. (d) Normalized ECSA values remaining for PtCoNW during ADT with commercial Pt/C provided for comparison. (inset) CV polarization data collected intermittently during ADT for PtCoNWs.

PtCoNWs in comparison to commercial Pt/C, along with improved ECSA retention (75% vs. 59%, respectively) measured through ADT cycling. A 65% increase in Pt mass based activity was also obtained for PtCoNWs in comparison to Pt/C, despite the relatively low surface area arising from the thick diameter of these nanowire catalysts. It is expected that further mass activity improvements can be achieved by careful control of the morphology (i.e. diameter) and atomic compositions of the PtCoNWs, capabilities that have been demonstrated herein by the versatile electrospinning technique. This provides a valuable platform for systematic structure-property investigations and optimization in order to combine the specific activity enhancements observed for extended Pt-alloy surfaces with increased Pt utilization by nanostructure control strategies, with the ultimate goal of preparing highly active, operationally stable 1D Pt-alloy nanowires to potentially replace conventional nanoparticle catalysts.

Acknowledgments

This work was supported by the University of Waterloo and the Waterloo Institute for Nanotechnology. TEM imaging was carried out at the Canadian Center for Electron Microscopy (CCEM) located at McMaster University. This research was conducted as part of the Catalysis Research for Polymer Electrolyte Fuel Cells (CaRPE FC) Network administered from Simon Fraser University

and supported by Automotive Partnership Canada (APC) Grant no. APCPJ 417858-11 through the Natural Sciences and Engineering Research Council of Canada (NSERC).

Appendix A. Supporting information

Supplementary data associated with this article can be found in the online version at http://dx.doi.org/10.1016/j.nanoen.2014.09.013.

References

[1] B. James, J. Kalinoski, K. Baum, Department of Energy Hydrogen Program Review – Manufacturing Cost Analysis of Fuel Cell Systems (2011), available online at: ⟨http://www.hydrogen.energy.gov/pdfs/review11/fc018_james_2011_o.pdf⟩.
[2] Y. Chen, J. Wang, H. Liu, R. Li, X. Sun, S. Ye, S. Knights, Electrochem. Commun. 11 (2009) 2071–2076.
[3] R. Borup, J. Meyers, B. Pivovar, Y.S. Kim, R. Mukundan, N. Garland, D. Myers, M. Wilson, F. Garzon, D. Wood, Chem. Rev. 107 (2007) 3904–3951.
[4] Y. Lu, Y. Jiang, W. Chen, Nano Energy 2 (2013) 836–844.
[5] United States Department of Energy, Technical Plan – Fuel Cells, 2012, available online at: ⟨http://www1.eere.energy.gov/hydrogenandfuelcells/mypp/pdfs/fuel_cells.pdf⟩.
[6] M.K. Debe, Nature 486 (2012) 43–51.
[7] D. Higgins, M.A. Hoque, M.H. Seo, R. Wang, F. Hassan, J.-Y. Choi, M. Pritzker, A. Yu, J. Zhang, Z. Chen, Adv. Funct. Mater 24 (2014) 4325–4336.
[8] D.C. Higgins, J.-Y. Choi, J. Wu, A. Lopez, Z. Chen, J. Mater. Chem. 22 (2012) 3727–3732.
[9] G. Wu, K.L. More, C.M. Johnston, P. Zelenay, Science 332 (2011) 443–447.
[10] Z. Chen, D. Higgins, A. Yu, L. Zhang, J. Zhang, Energy Environ. Sci. 4 (2011) 3167–3192.
[11] C. Kok Poh, S. Hua Lim, Z. Tian, L. Lai, Y. Ping Feng, Z. Shen, J. Lin, Nano Energy 2 (2013) 28–39.
[12] C. Chen, Y. Kang, Z. Huo, Z. Zhu, W. Huang, H.L. Xin, J.D. Snyder, D. Li, J.A. Herron, M. Mavrikakis, M. Chi, K.L. More, Y. Li, N.M. Markovic, G.A. Somorjai, P. Yang, V.R. Stamenkovic, Science 343 (2014) 1339–1343.
[13] B.Y. Xia, H.B. Wu, Y. Yan, X.W. Lou, X. Wang, J. Am. Chem. Soc. 135 (2013) 9480–9485.
[14] B.Y. Xia, H.B. Wu, X. Wang, X.W. Lou, Angew. Chem. Int. Ed. 52 (2013) 12337–12340.
[15] C. Koenigsmann, W.-p. Zhou, R.R. Adzic, E. Sutter, S.S. Wong, Nano Lett. 10 (2010) 2806–2811.
[16] Q. Li, P. Xu, B. Zhang, G. Wu, H. Zhao, E. Fu, H.-L. Wang, Nanoscale 5 (2013) 7397–7402.
[17] G. Zhang, S. Sun, M. Cai, Y. Zhang, R. Li, X. Sun, Sci. Rep. 3 (2013).
[18] S. Sun, G. Zhang, Y. Zhong, H. Liu, R. Li, X. Zhou, X. Sun, Chem. Commun. (2009) 7048–7050.
[19] Y. Bing, H. Liu, L. Zhang, D. Ghosh, J. Zhang, Chem. Soc. Rev. 39 (2010) 2184–2202.
[20] Z. Chen, M. Waje, W. Li, Y. Yan, Angew. Chem. Int. Ed. 46 (2007) 4060–4063.
[21] S. Sun, G. Zhang, D. Geng, Y. Chen, R. Li, M. Cai, X. Sun, Angew. Chem. Int. Ed. 123 (2011) 442–446.
[22] B.Y. Xia, W.T. Ng, H.B. Wu, X. Wang, X.W. Lou, Angew. Chem. Int. Ed. 124 (2012) 7325–7328.
[23] V.T.T. Ho, N.G. Nguyen, C.-J. Pan, J.-H. Cheng, J. Rick, W.-N. Su, J.-F. Lee, H.-S. Sheu, B.-J. Hwang, Nano Energy 1 (2012) 687–695.
[24] A.L. Tiano, C. Koenigsmann, A.C. Santulli, S.S. Wong, Chem. Commun. 46 (2010) 8093–8130.
[25] R. Wang, D.C. Higgins, M.A. Hoque, D. Lee, F. Hassan, Z. Chen, Sci. Rep. 3 (2013).
[26] S. Sun, F. Jaouen, J.-P. Dodelet, Adv. Mater. 20 (2008) 3900–3904.
[27] Z. Zhang, M. Li, Z. Wu, W. Li, Nanotechnology 22 (2011) 015602.
[28] D.C. Higgins, S. Ye, S. Knights, Z. Chen, Electrochem. Solid, St, Letters 15 (2012) B83–B85.
[29] R. Wang, C. Xu, X. Bi, Y. Ding, Energy Environ. Sci. 5 (2012) 5281–5286.
[30] N.V. Long, Y. Yang, C. Minh Thi, N.V. Minh, Y. Cao, M. Nogami, Nano Energy 2 (2013) 636–676.
[31] C. Koenigsmann, M.E. Scofield, H. Liu, S.S. Wong, J. Phys. Chem. Lett. 3 (2012) 3385–3398.
[32] D. Li, Y. Wang, Y. Xia, Nano Lett. 3 (2003) 1167–1171.
[33] H.J. Kim, Y.S. Kim, M.H. Seo, S.M. Choi, W.B. Kim, Electrochem. Commun. 11 (2009) 446–449.
[34] J. Wu, H.W. Park, A. Yu, D. Higgins, Z. Chen, J. Phys. Chem. C 116 (2012) 9427–9432.
[35] J.-l. Shui, C. Chen, J.C.M. Li, Adv. Funct. Mater. 21 (2011) 3357–3362.
[36] V.R. Stamenkovic, B.S. Mun, M. Arenz, K.J.J. Mayrhofer, C.A. Lucas, G. Wang, P.N. Ross, N.M. Markovic, Nat. Mater. 6 (2007) 241–247.
[37] D. van der Vliet, D.S. Strmcnik, C. Wang, V.R. Stamenkovic, N.M. Markovic, M.T.M. Koper, J. Electroanal. Chem. 647 (2010) 29–34.
[38] D.C. Higgins, D. Meza, Z. Chen, J. Phys. Chem. C 114 (2010) 21982–21988.
[39] Y. Garsany, O.A. Baturina, K.E. Swider-Lyons, S.S. Kocha, Anal. Chem. 82 (2010) 6321–6328.
[40] D. Wang, H.L. Xin, R. Hovden, H. Wang, Y. Yu, D.A. Muller, F.J. DiSalvo, H.D. Abruña, Nat. Mater. 12 (2013) 81–87.
[41] B.P. Vinayan, R. Nagar, N. Rajalakshmi, S. Ramaprabhu, Adv. Funct. Mater. 22 (2012) 3519–3526.
[42] K.C. Neyerlin, B.A. Larsen, S. Pylypenko, S.S. Kocha, B.S. Pivovar, ECS Trans. 50 (2013) 1405–1413.
[43] I.E.L. Stephens, A.S. Bondarenko, U. Gronbjerg, J. Rossmeisl, I. Chorkendorff, Energy Environ. Sci. 5 (2012) 6744–6762.
[44] H.A. Gasteiger, S.S. Kocha, B. Sompalli, F.T. Wagner, Appl. Catal. B 56 (2005) 9–35.
[45] K.J.J. Mayrhofer, D. Strmcnik, B.B. Blizanac, V. Stamenkovic, M. Arenz, N.M. Markovic, Electrochim. Acta 53 (2008) 3181–3188.

Drew Higgins is a Ph.D. student in Chemical Engineering at the University of Waterloo working under the supervision of Dr. Zhongwei Chen, and a Visiting Scholar at the Los Alamos National Laboratory. His research focuses on the development of nanostructured electrode materials for fuel cell and battery technologies. He has currently published one book chapter and more than 50 peer-reviewed journal articles that have received over 1300 citations to date.

Rongyue Wang is a Guest Researcher in the Material Science & Engineering Division at the National Institute of Standards and Technology. He received his Ph.D. degree in Chemistry from Shandong University in 2012 and worked with Professor Zhongwei Chen at the University of Waterloo as a Postdoctoral Fellow in 2012 and 2013. His research interests are ranging from nanomaterial synthesis to fundamental electrochemistry related to energy conversion and storage techniques such as fuel cells, batteries, capacitors and photoelectrochemical devices.

Md. Ariful Hoque is currently doing his Ph. D. in Chemical Engineering at the University of Waterloo, Canada. He obtained his MASc in Chemical Engineering from Yeungnam University, South Korea and B.Sc. in Chemical Engineering from Bangladesh University of Engineering and Technology (BUET), Bangladesh. His research focuses on the development of heteroatom-doped carbon nanostructures as platinum supports for fuel cell applications.

Pouyan Zamani received his Bachelor's degree in Polymer Engineering (2007) and Master's degree in Polymer/Nanotechnology Engineering (2010) from Amirkabir University (Tehran Polytechnic). He then joined the Engineering Research Institute in Tehran as a researcher. He is now a Ph.D. student in Chemical Engineering at the University of Waterloo under the supervision of Dr. Zhongwei Chen, with a focus on the development of nanostructured carbon based materials as non-precious catalysts for fuel cell applications.

Salah Abureden is a Ph.D. student in Chemical Engineering at the University of Waterloo working under the supervision of Dr. Zhongwei Chen. His research focuses on the development of advanced lithium titanate nanostructured materials for energy storage technologies.

Zhongwei Chen is an Associate Professor of Chemical Engineering at the University of Waterloo. His research interests are the development of advanced electrode materials for metal-air batteries, lithium-ion batteries and fuel cells. He received his Ph.D. in Chemical and Environmental Engineering from the University of California-Riverside. Prior to joining Waterloo in 2008, he focused on advanced catalyst research at the Los Alamos National Laboratory. He has published 1 book, 4 book chapters and more than 90 peer-reviewed journal articles that have been cited over 4000 times. He is an inventor on 3 US patents and 8 provisional US patents, with two licensed to startup companies in USA.